Annual Performance Report
for the period 15 April 1995 - 14 April 1996

for

NASA Grant No. NAG 5-2927

entitled

EVALUATING AND UNDERSTANDING PARAMETERIZED CONVECTIVE PROCESSES AND THEIR ROLE IN THE DEVELOPMENT OF MESOSCALE PRECIPITATION SYSTEMS

submitted to

Ms. Gloria R Blanchard
Grants Officer
NASA/Goddard Space Flight Center
Code 286.1
Greenbelt MD 20771

by

J. Michael Fritsch
Principal Investigator
Department of Meteorology

and

John S. Kain
Co-Principal Investigator
Department of Meteorology

The Pennsylvania State University
Office of Sponsored Programs
110 Technology Center
University Park PA 16802

March 5, 1996

Evaluating and Understanding Parameterized Convective Processes and Their Role in the Development of Mesoscale Precipitation Systems.

NASA Grant NAG 5-2927
First Year (3/1/95 - 2/29/96) Annual Report
John S. Kain and J. Michael Fritsch
Department of Meteorology
Pennsylvania State University

I. Summary of Progress

Research efforts during the first year focused on numerical simulations of two convective systems with the Penn State/NCAR mesoscale model. The first of these systems was tropical cyclone Irma, which occurred in 1987 in Australia's Gulf of Carpentaria during the AMEX field program. Comparison simulations of this system were done with two different convective parameterization schemes (CPSs), the Kain-Fritsch (1993 - KF) and the Betts-Miller (Betts 1986 - BM) schemes. The second system was the June 10-11 1985 squall line simulation, which occurred over the Kansas-Oklahoma region during the PRE-STORM experiment. Simulations of this system using the KF scheme were examined in detail.

A. Tropical cyclone Irma

Tropical cyclone Irma formed within an array of upper-air-observation sites that was in place for the AMEX study, allowing initial conditions to be exceptionally well-defined for a case of tropical cyclone genesis. Simulations were performed with the hydrostatic version of the PSU/NCAR model. The model was configured with a two-way interactive nested grid, a 75 km grid length on the coarse mesh, and 25 km grid length on the fine mesh. Grid-resolved precipitation processes were represented with prognostic equations for cloud water, cloud ice, rain, and snow, while a high-resolution Blackadar (1979) planetary boundary layer scheme (Zhang and Anthes 1982) was used..

The domain of the coarse-mesh grid (not shown) extends from the equator southward to 30° S latitude, while spanning the entire Australian continent and nearby ocean areas in the zonal direction. The domain covered by the fine-mesh grid, centered on the region where tropical cyclogenesis occurs, is shown along with initial surface meteorological conditions in Fig. 1. At the initial time, a weak mid-level vortex is present over the northeastern Gulf of Carpentaria, and this is reflected in the surface wind field as a cyclonic circulation (Fig. 1).

Our investigation focused on the analysis of two 48 h simulations, one using the KF scheme and the other using the BM scheme. At the 48 hour time, the central pressure of the cyclone in the two integrations was nearly identical (cf. Figs. 2a and 3a), but the structure and evolution of the two simulated systems were quite different. For example, the circulation center in the KF simulation was about 175 km to the southwest of the BM system and it tilted significantly to the north with height; the BM system was more consistent with the observed location of Irma and had very little tilt with height.

A significant difference in the evolution of the two systems was related to the partitioning of precipitation between parameterized and explicitly-resolved production mechanisms. Both CPSs initially generated precipitation near the circulation center at a rate of about 1 cm h^{-1}. However, by the end of the first hour, grid-resolved precipitation had developed in the KF run, but not in the BM run. By the 6 h time, resolved precipitation rates in the KF simulation had risen to over 3 cm h^{-1} over a very small area (2 - 4 δx) near the circulation center. This intense rainfall was embedded within a larger region of steady parameterized precipitation, accumulating at a rate of 0.5 to 1 cm h^{-1}. In contrast, maximum parameterized precipitation rates from the BM scheme averaged 1 - 1.5 cm h^{-1} during this time, but no significant grid-resolved precipitation developed. This disparity in precipitation characteristics continued throughout the simulation. At the 48 h time, grid-resolved latent heating was very strong near the circulation center in the KF simulation (Fig. 2b) but relatively weak in the BM simulation (Fig. 3b).

The emergence of explicitly-resolved precipitation has significant implications in this type of simulation. Specifically, it changes both the vertical and horizontal distributions of latent heating, which are known to strongly influence the dynamical evolution of developing cyclones (e.g., Hack and Schubert 1986). Because of the potential impact of resolved precipitation processes, considerable effort was expended to determine which parameters in these two CPSs modulate convective intensity and the transition between the different precipitation-production mechanisms.

1.) The Kain-Fritsch scheme

A detailed analysis of the KF simulation revealed that intense localized upward motions developed at grid points where saturation developed before the KF scheme had eliminated conditional instability. The KF scheme is formulated to reflect the assumption that vertical stabilization of a grid element occurs over a time period comparable to the life cycle of a single deep convective cloud, 0.5 to 1 hour. It computes a convective-scale mass flux that would completely eliminate CAPE for a subcloud source layer 50-100 mb deep. It accomplishes this stabilization by removing high-θ_e, unstable air, from this layer in parameterized updrafts and replacing it with relatively low-θ_e downdraft air. Through this mechanism, the KF scheme is effective at greatly reducing the convective potential of the *original updraft-source layer*. Above this source layer, however, the scheme's stabilizing effect is much weaker. Thus, if a deep layer of instability exists, the portion of this layer that is not directly modified by the parameterized detrainment of downdraft air can become saturated by larger-scale processes while it is still conditionally unstable. The resultant structure is *absolutely* unstable. This type of instability (Fig. 4) preceded the development of intense vertical motions and excessive localized precipitation rates in the KF simulation.

In order to alter this process, the KF scheme was modified so that multiple clouds could develop in individual grid columns. In particular, each model layer was evaluated independently as a potential updraft source layer and the downdraft associated with any updraft was constrained to detrain all of its mass in this source layer. This procedure provided a mechanism to allow for an efficient and simultaneous stabilization of multiple model layers.

This modification proved to be very effective at preventing the development of absolutely unstable layers and a simulation with the modified scheme produced only trace amounts of grid-scale rainfall. However, parameterized convective precipitation rates decreased significantly in

this simulation as well, and the cyclone showed only minimal intensification by 48 h. Examination of this integration suggested that the modified convection algorithm was too efficient at stabilizing the atmosphere i.e., CAPE in the model atmosphere was removed without enough latent heat release to induce significant surface pressure falls. Thus, numerous systematic variations of this multiple-cloud procedure were tested, with parametric adjustments designed to control the net rate of convective overturning and the level of partitioning between subgrid-scale (parameterized) and grid-scale precipitation. This testing revealed that intensification rates in the KF simulations were strongly correlated with resolved-scale precipitation rates. In particular, higher grid-scale precipitation rates were associated with more rapid intensification.

Consistent with this correlation, it was found that simulations with the KF scheme were most sensitive to parameters that control the net convective moistening rate. One component of the KF scheme that has the potential to significantly affect the net moistening rate is the parameterized downdraft. The downdraft tends to induce a moistening tendency in the lower part of the cloud layer because its downward transport of mass must be compensated by upward motion in the cloud environment within the KF scheme. This compensating mass flux typically results in an upward transport of moisture in this layer. Thus, increased downdraft mass flux favors the development of a saturated layer in the lower troposphere where conditional instability is prevalent, increasing the potential for a strong grid-scale response.

The downdraft mass flux can be adjusted by one of two ways in the KF scheme. The first way is to modify the calculation of precipitation efficiency in the scheme. This parameter regulates the fractional amount of the total condensate produced by the updraft that will be available to evaporate in the downdraft. For example, a higher precipitation efficiency leaves less condensate available for evaporation, forcing a reduction in the downdraft mass flux. The second method involves modifications to the procedure for selecting the downdraft initiation level, labeled the level of free sink (LFS) in the scheme . For example, a lower LFS reduces the depth of the downdraft and, for a fixed availability of condensate for evaporation, a larger downdraft mass flux.

The interactions between parameterized convective feedbacks and grid-scale circulations are quite complex and highly non-linear, and other factors were clearly affecting the development of these unstable structures. Significantly, however, every simulation in which significant cyclone development occurred with the KF scheme involved a grid-scale response to absolutely unstable vertical structures, i.e., a grid-scale manifestation of convective overturning. Thus, this response appeared to be an essential part of the deepening process. The most realistic simulations with the KF scheme seemed to achieve a delicate, quasi-balanced development involving a controlled grid-scale response to this instability, large-scale destabilization, and parameterized convective feedbacks.

2.) The Betts-Miller Scheme

Grid-resolved precipitation rates in the simulation with the BM scheme were generally much smaller than those produced in the KF runs. In fact, during much of the 48 h simulation, resolved rainfall was negligible in the vicinity of the circulation center. However, there was a critical time period, from about 12 to 24 hours into the simulation, when resolved precipitation rates exceeded 1 cm h^{-1} at isolated grid points and unstable grid-scale structures and responses were very similar to those seen in the KF simulations. The strong upward motions associated

with these structures developed at the circulation center and were accompanied by a drop in surface pressure from 1007 mb to 1004 mb. This pressure drop, although rather small in an absolute sense, marked the transition of the surface pressure field from a largely flat pattern with a slight, amorphous depression near the circulation center to a well-defined circular surface low with two closed-millibar contours. Thus, the genesis stage of the BM simulation was clearly associated with a grid-resolved overturning process similar to that observed in the KF run, suggesting that this process is a critical element of the intensification of simulated systems when this scheme is used as well.

Resolved precipitation rates near the circulation center dropped off rapidly as the simulation approached the 24 h time and as alluded to above, remained insignificant (less than 0.01 cm h^{-1}) before increasing modestly just prior to the 48 h time. Nonetheless, the central pressure of the cyclone dropped steadily during this time period, evidently driven by parameterized heating alone. Thus, unlike the simulations with the KF scheme, intensification of the simulated system beyond the genesis stage did *not* appear to require grid-scale latent heating.

Previous studies (e.g., Baik et al. 1990) have shown that the level of partitioning between parameterized and grid-resolved latent heating in this type of environment can be changed by modifying the convective adjustment time in the BM scheme. Specifically, when the adjustment time is lengthened, convective heating and drying rates are decreased, increasing the likelihood that grid-scale saturation and precipitation will occur before conditional instability is removed. In a sensitivity test with the BM scheme, the adjustment time scale was changed from 3000 s to 7200 s. This simulation did produce higher grid-resolved precipitation rates, but unlike the KF runs, the resolved heating maxima were not co-located with the circulation center. Furthermore, the central pressure of the simulated system had only dropped to 1005 mb by the 48 h time, compared with 994 mb in the control run (Fig. 3a). Thus, any correlation between cyclone intensity and grid-resolved precipitation rates was less obvious when the BM scheme was used.

B. The June 10-11 Squall Line

The June 10-11 1985 squall line is an exceptionally well-documented MCS that has been successfully simulated by several investigators (e.g., Zhang et al. 1989; Grell 1993). We emulated previous simulations of this case for the purpose of identifying the elements of the modeling system's representation of deep convection that were most important in generating a realistic simulation. In particular, we used a model configuration and initial condition identical to Zhang et al. (1989 - ZGP), with the one exception being that we used the KF scheme on the fine mesh grid whereas ZGP used the Fritsch-Chappell (1980 - FC) scheme.

The KF scheme was developed within the framework of the FC parameterization, but unlike the FC scheme, it was designed to conserve mass, moisture, and thermal energy. However, in early testing it was found that when conservation principles were imposed in the KF scheme so that computations deviated from the original FC approach, the quality of the June 10-11 squall line simulation suffered. In particular, when the simulation was run with conservation imposed, the southern flank of the system was considerably weaker and propagated more slowly (compare Figs. 4a and b), in poorer agreement with observations.

An in-depth analysis of this tendency revealed the underlying cause for the difference, as described below. The original FC scheme is non-conservative because it is formulated such that updraft mass fluxes, and compensating environmental subsidence, are not computed below cloud

base. More specifically, they are not continued below cloud base and down to the source layers for the updraft air, resulting in an under-estimation of sub-cloud layer drying effects compared to a mass-conservative calculation. A significant consequence of the non-conservative approach is that more moisture is available in the low levels during, and following, a convective cycle, increasing the chances that a second, reinforcing cycle will be initiated and/or the grid-scale environment will become saturated before conditional instability is removed. Consistent with this effect, when updraft mass flux and compensating subsidence calculations were made only at cloud base and above in the KF scheme, the simulated results agreed better with ZGP's results and observations of this case. Thus the KF scheme was kept in a non-conservative configuration for this testing. It should be recognized, however, that this sensitivity is in itself an important result.

As was deduced in the simulation of tropical cyclone Irma, grid-scale latent heat release was found to be a critically important component of the June 10-11 squall line simulation. At the 9 hour time of this simulation, the convective line was realized almost entirely as a parameterized feature. However, over the next six hours both the areal coverage and intensity of grid-scale rainfall increased rapidly (Fig. 5) as the convective system reached its mature stage. Over that portion of the simulated line where mesoscale circulations were strongest and the most distinctive perturbations developed, precipitation processes followed a characteristic sequence as the disturbance passed overhead. Specifically, precipitation began as subgrid-scale, parameterized convection, quickly became a mixture of parameterized convection and grid-resolved rainfall, and eventually ended as a period of resolved precipitation only.

It was during the intermediate stage of development, when parameterized and explicitly-resolved precipitation processes were both active, that vertical circulations became most intense. As in the Irma case, an ubiquitous precursor to these intense vertical motions was the development of a moist, absolutely unstable vertical structure that formed because the grid-scale environment became saturated before the convective parameterization scheme had consumed all of the potential buoyant energy (e.g., see Fig. 6). The grid-scale response to this structure was a hydrostatic manifestation of deep convective overturning. Thus, deep convection was realized in the model as a combination of parameterized and explicitly resolved processes. Over much of the convective line, the mesoscale contribution to convective overturning rivaled, and often exceeded the parameterized contribution.

As with the simulations of Irma, numerous attempts were made to assure that conditional instability was removed before grid-scale latent heat release becomes significant. However, as with Irma, each modification of the KF scheme proved to be detrimental to the quality of the mesoscale simulation. This testing has led us to conclude that there are two important reasons why convection in these systems is best represented as a hybrid of parameterized feedbacks and grid-scale overturning. First, it must be acknowledged that CPSs are not designed to represent mesoscale circulations and interactions between convective clouds. Even the most sophisticated CPSs are very crude representations of the highly nonlinear processes involved in atmospheric convection. Existing schemes cannot represent convective clouds that slope with height; they handle momentum transports very poorly, if at all; the vertical distribution of heating and moistening effects are based on simplistic cloud models. Most importantly, they are not designed to represent the nonlinear interactions and organizational tendencies that characterize ensembles of precipitating convective clouds. These processes must be represented on resolved scales if they are to be represented at all because the full equations of motion provide continuity and all-encompassing effects that CPSs lack. Second, it appears that mesoscale circulations evolve in a

much more realistic manner when they are driven, at least in part, by the primary driving force for the whole system, i.e., convective instability. Within that component of the convective circulation that is manifested as grid-resolved overturning, upward (and eventually downward) motions are intimately linked to and inseparable from latent heat release. This combined evolution of the dynamic and thermodynamic fields is more consistent with what occurs in nature than a dynamical evolution based solely on grid-scale response to parameterized heating.

Many aspects of the way in which deep convective overturning is manifested in a mesoscale model are clearly artifacts of approximations involved in parameterizing convection and poor resolution of convective features. Nonetheless, for the currently available CPSs, it appears to be desirable to allow the slower modes of convective overturning to be explicitly represented on the mesoscale grid.

II. Work Plan: March 1,1996 - February 28, 1997

The work plan for the upcoming year will focus on satisfying the objectives established for year two in our original proposal.

A. Diagnosing and Analyzing Convective Feedback Rates in MM5

Our investigations during the current year have revealed important behavioral characteristics of the MM4 and MM5 modeling systems. In particular, it has been found that deep convection is represented in these modeling systems as both parameterized and explicitly resolved modes. Over the next year, the feedbacks associated with both of these processes will be analyzed. This analysis will involve comparisons of the magnitudes and vertical distributions of heating and drying feedbacks coming from both the parameterization schemes and resolved phase changes. In addition, the characteristics of the grid-scale response to these different feedbacks will be diagnosed.

Numerous users of the MM5 modeling system (e.g., Wang and Seaman 1996; Kuo et al. 1996) have found that the KF and BM schemes tend to give the most realistic results. Therefore, our investigations over the next year will concentrate on these two schemes.

B. Implementation and Testing of the KF, BM, and Grell Schemes in the GCE Model

The interface parameters required by the KF, BM, and Grell schemes have been identified so that these schemes are ready to implement in the GCE. We will assist with this implementation as needed. Once the implementation is complete, we will begin comparisons of parameterized heating and drying tendencies with those produced in explicit simulations of the same convective systems by the GCE.

III. Publications During Year 1

Kain, J.S., and J.M. Fritsch, 1996: Multiscale Convective Overturning in Mesoscale Convective Systems: Reconciling Observations, Simulations, and Theory. Submitted to *Monthly Weather Review*.

Wang, Y., W.-K. Tao, K.E. Pickering, A.M. Thompson, J.S. Kain, R.F. Adler, J. Simpson, P.R. Keehn, and G.S. Lai, 1996: Mesoscale model simulations of TRACE-A and PRE-STORM convective systems and associated tracer transport. *Journal of Geophysical Research,* in press.

References

Baik, J.-J., M. DeMaria, and S. Raman, 1990: Tropical cyclone simulations with the Betts convective adjustment scheme. Part II: Sensitivity experiments. *Mon. Wea. Rev.*, **118**, 529-541.

Betts, A.K., 1986: A new convective adjustment scheme. Part I: Observational and theoretical basis. *Quart. J. Roy. Meteor. Soc.*, **112**, 677-692.

Blackadar, A.K., 1979: High resolution models of the planetary boundary layer. *Advances in Environmental Science and Engineering*, 1, No. 1, Pfafflin and Ziegler, Eds., Gordon and Briech Sci. Publ., New York, 50-85.

Fritsch, J.M., and C.F. Chappell, 1980a: Numerical prediction of convectively driven mesoscale pressure systems. Part I: Convective parameterization. *J. Atmos. Sci.*, **37**, 1722-1733.

Grell, G.A., 1993: Prognostic evaluation of assumptions used by cumulus parameterizations. *Mon. Wea. Rev.*, **121**, 764-787.

Hack, J.J., and W.H. Schubert, 1986: Nonlinear response of atmospheric vortices to heating by organized cumulus convection. *J. Atmos. Sci.*, **43**, 1559-1573.

Kain, J.S., and J.M. Fritsch, 1993: Convective parameterization for mesoscale models: The Kain-Fritsch scheme. *The representation of cumulus convection in numerical models. Meteor. Monogr., No. 24*, Amer. Meteor. Soc., 165-170.

Kuo, Y.-H., R.J. Reed, and Y.Liu, 1996: The ERICA IOP5 storm: Mesoscale cyclogenesis and precipitation parameterization. Submitted to *Mon. Wea. Rev.*

Wang, W., and N.L. Seaman, 1996: A comparison study of convective parameterization schemes in a mesoscale model. submitted to *Mon. Wea. Rev.*

Zhang, D.-L., and R.A. Anthes, 1982: A high resolution model of the planetary boundary layer - sensitivity tests and comparisons with SESAME-79 data. *J. Appl. Meteor.*, **21**, 1594-1609.

Zhang, D.-L., K. Gao, and D.B. Parsons, 1989: Numerical simulation of an intense squall line during 10-11 June 1985 PRE-STORM. Part I: Model verification. *Mon. Wea. Rev.*, **117**, 960-994.

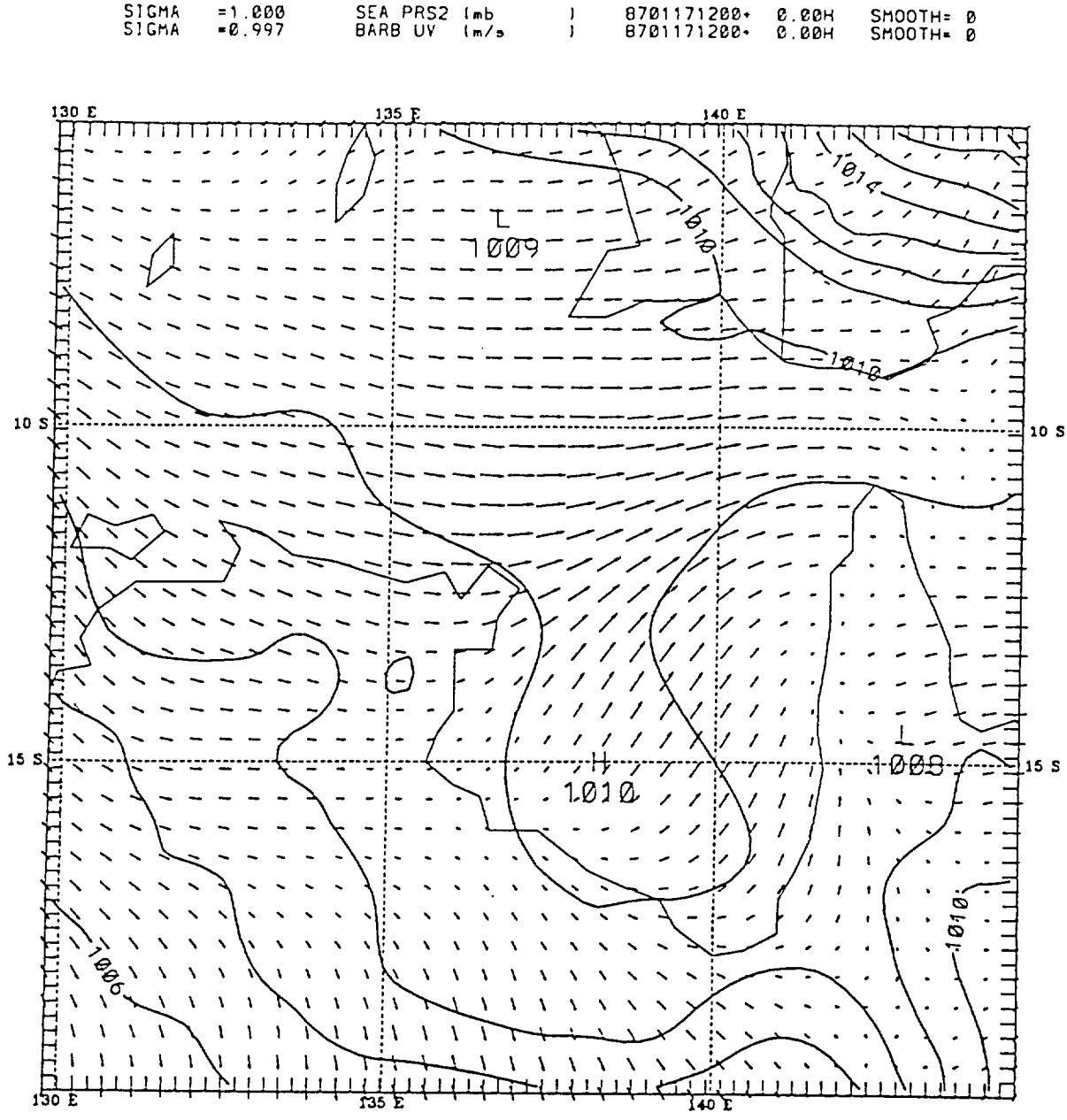

Fig. 1 Initial conditions over the fine-mesh domain for the Irma simulations, valid 1200 UTC 17 January 1987, showing sea-level pressure (contour interval = 1 mb) and surface-layer wind vectors (maximum vector = 10.6 m s^{-1}).

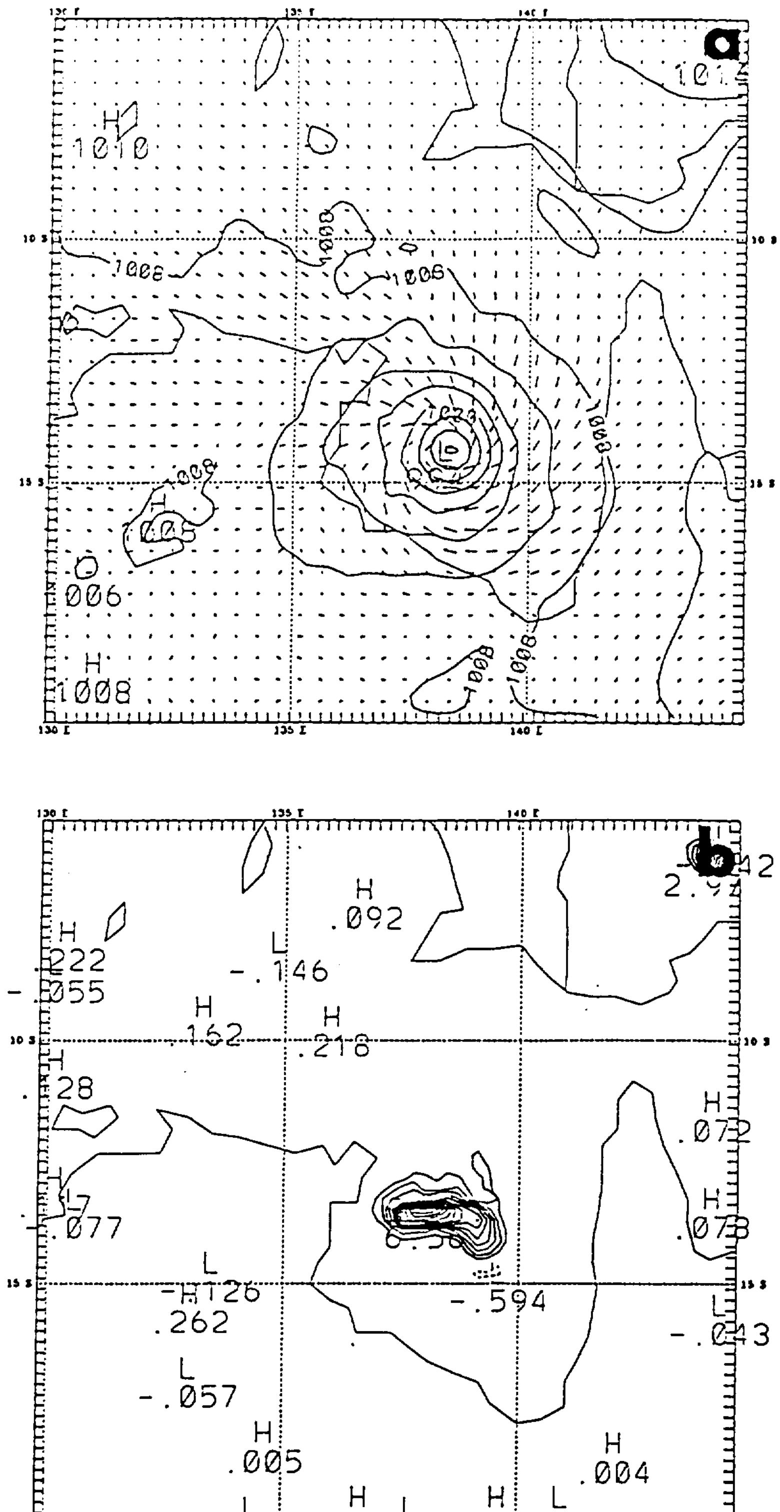

Fig. 2 Results from the 48 h time of the Irma simulation using the KF scheme showing (a) sea-level pressure (2 mb contour interval) and surface-layer wind vectors (maximum vector = 24.5 m s^{-1}) and (b) vertically integrated grid-scale latent heating (contour interval = 0.5 K h^{-1})

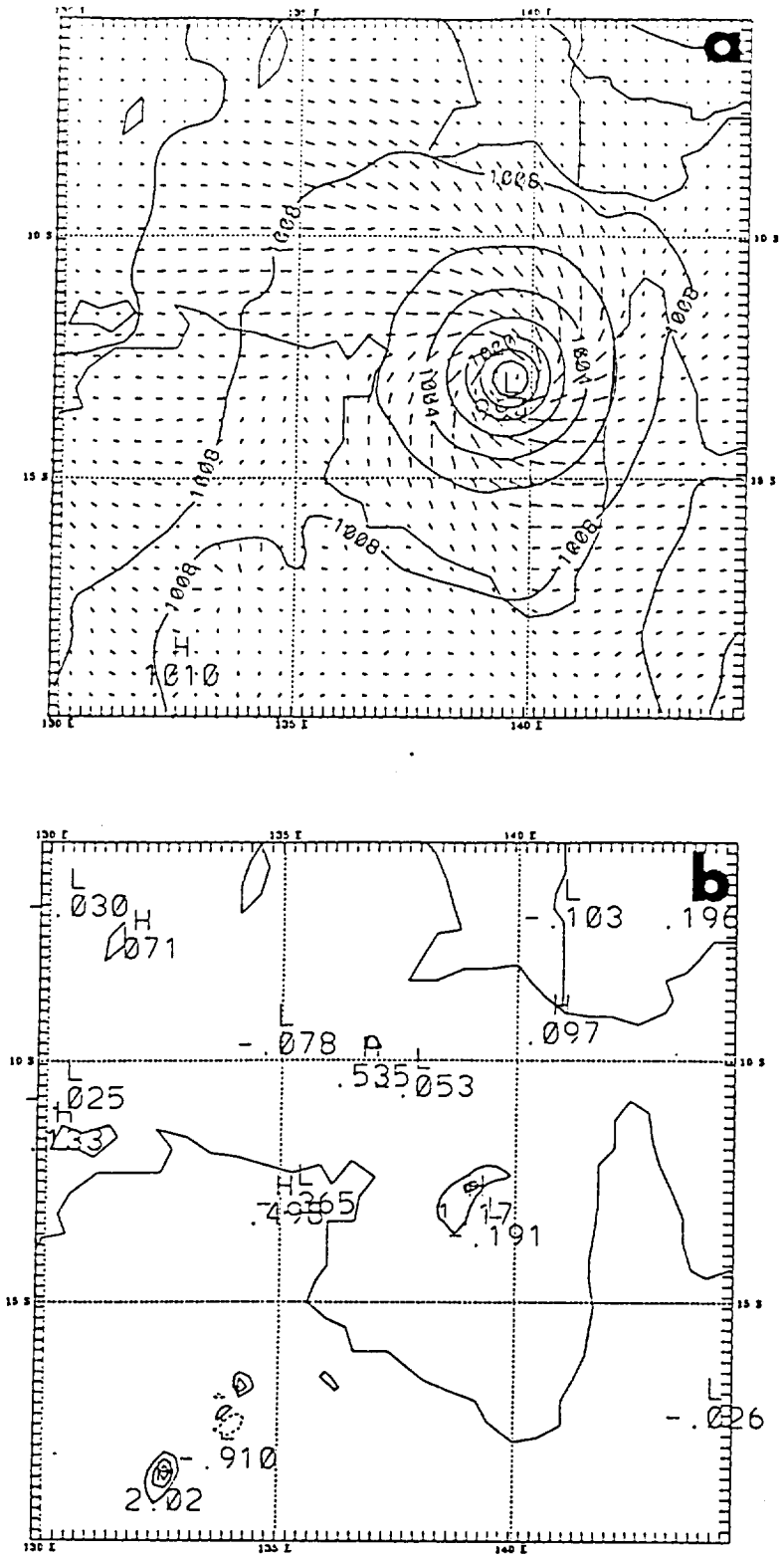

Fig. 3 Results from the 48 h time of the Irma simulation using the BM scheme showing (a) sea-level pressure (2 mb contour interval) and surface-layer wind vectors (maximum vector = 21.9 m s^{-1}) and (b) vertically integrated grid-scale latent heating (contour interval = 0.5 K h^{-1})

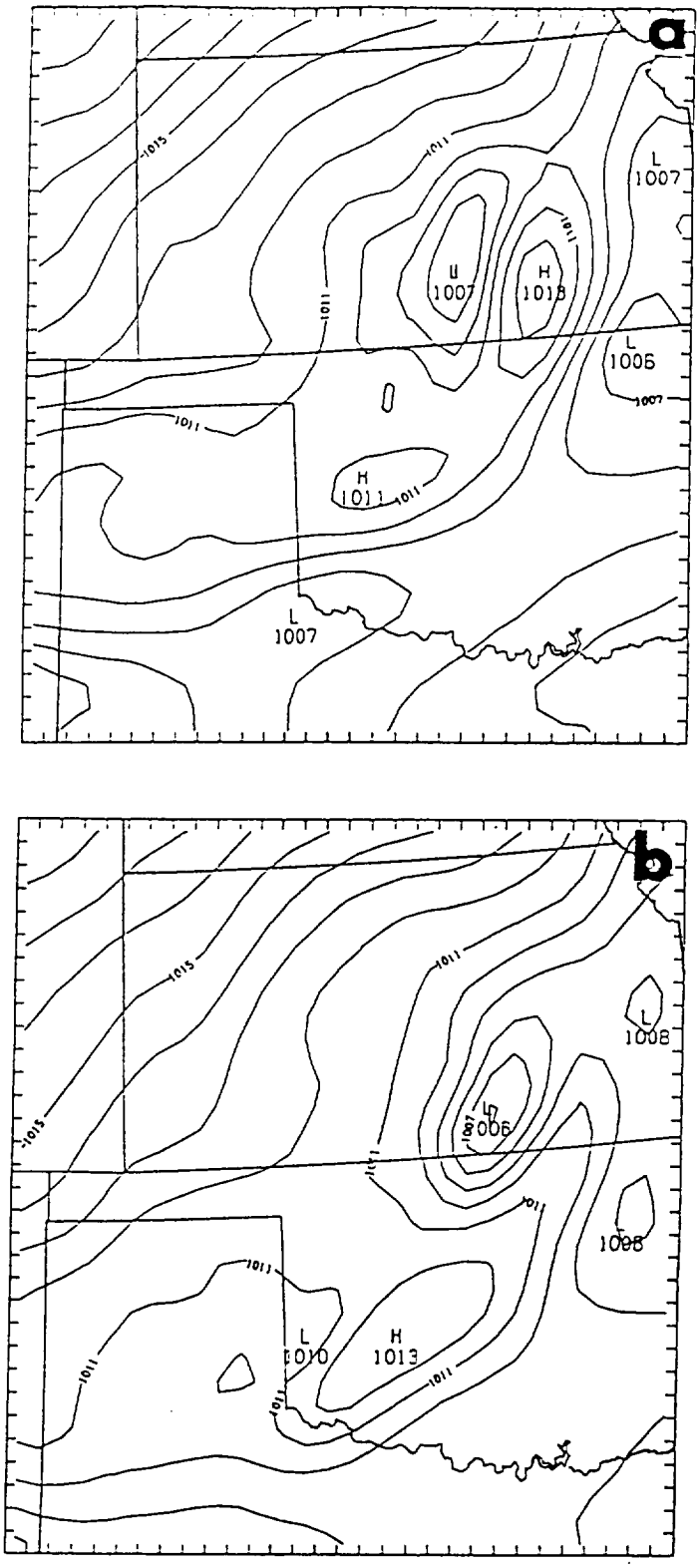

Fig. 4 Sea-level pressure (1 mb contour interval) at the 18 h time for simulations of the June 10-11 squall line using (a) a mass conservative and (b) a non-conservative formulation in the KF scheme.

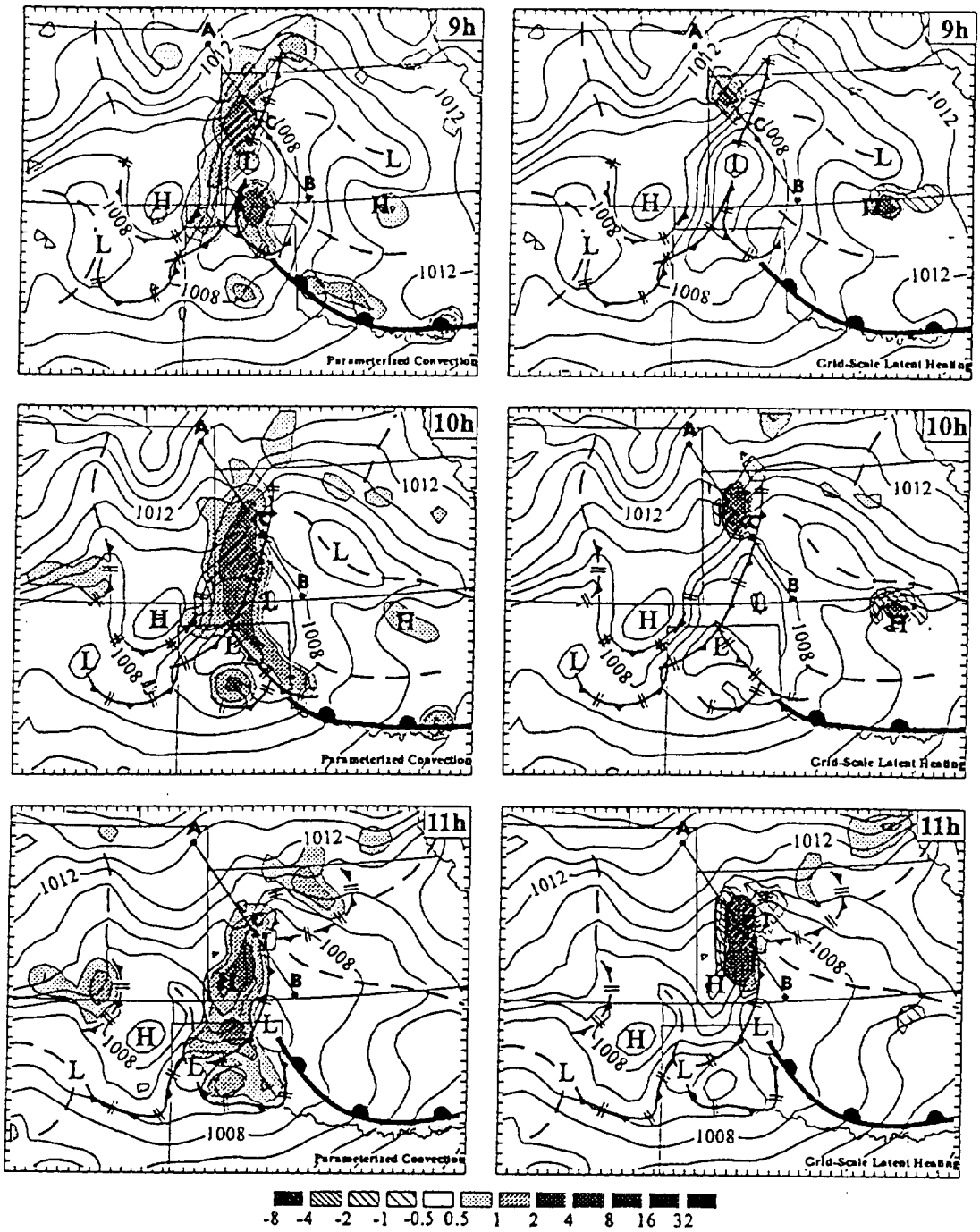

Fig. 5 June 10-11 squall line simulation results from the 9 hr to 15 hr time period, showing sea-level pressure (contour interval 1 mb) with vertically-integrated parameterized convective heating (left-hand-side) and vertically-integrated grid-scale latent heating (right-hand-side). Intensity of the heating is indicated by the shading scale at the bottom. Points A and B in hours 9-11 mark the endpoints of vertical cross section analyses (not shown). Point C marks the location of the sounding shown in Fig. 6.

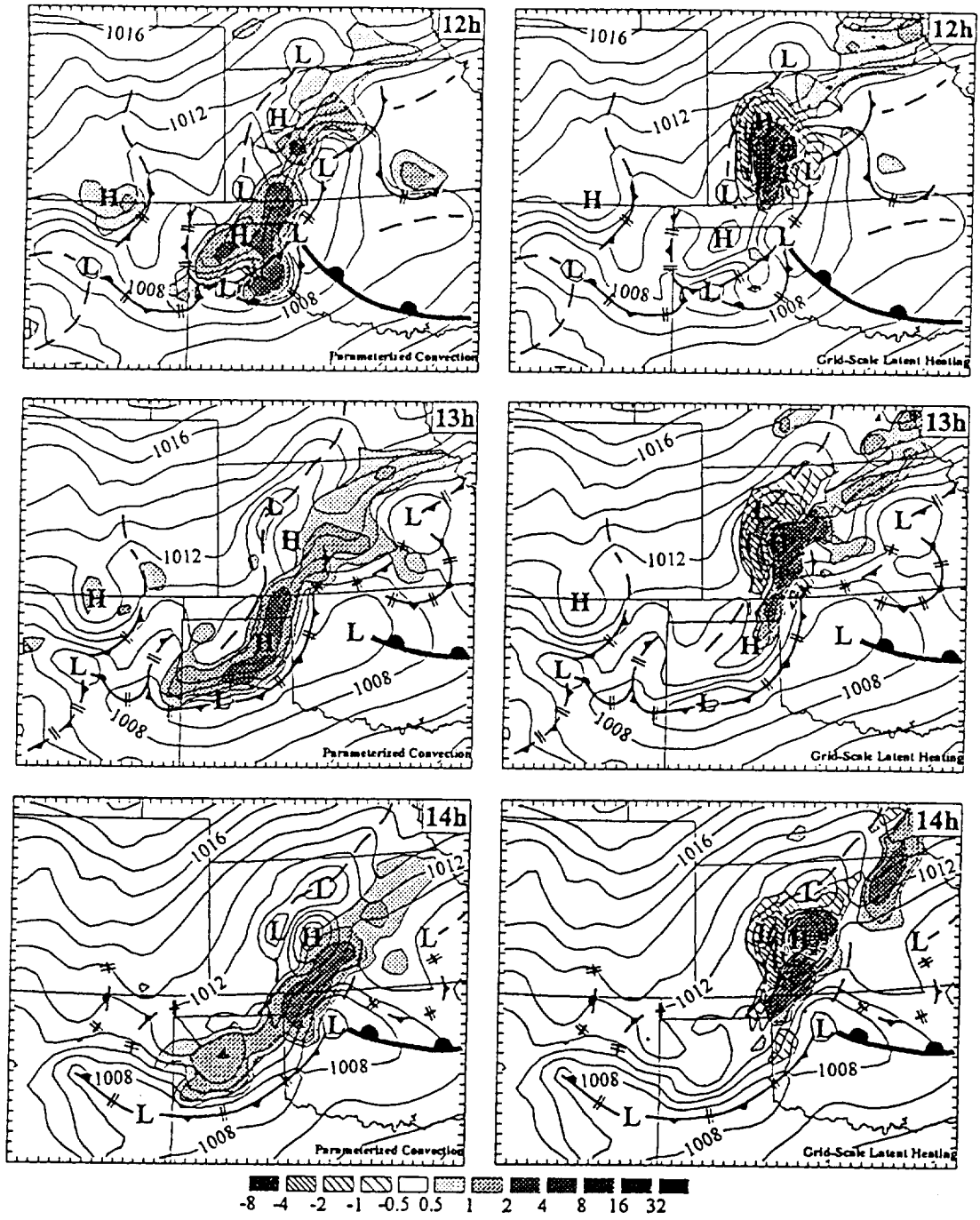

Fig. 5 (continued)

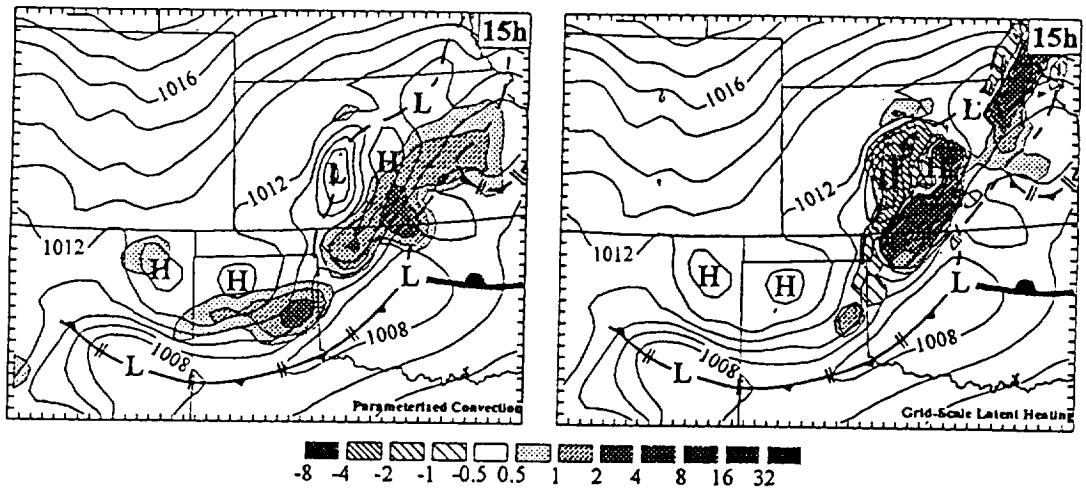

Fig. 5 (continued)

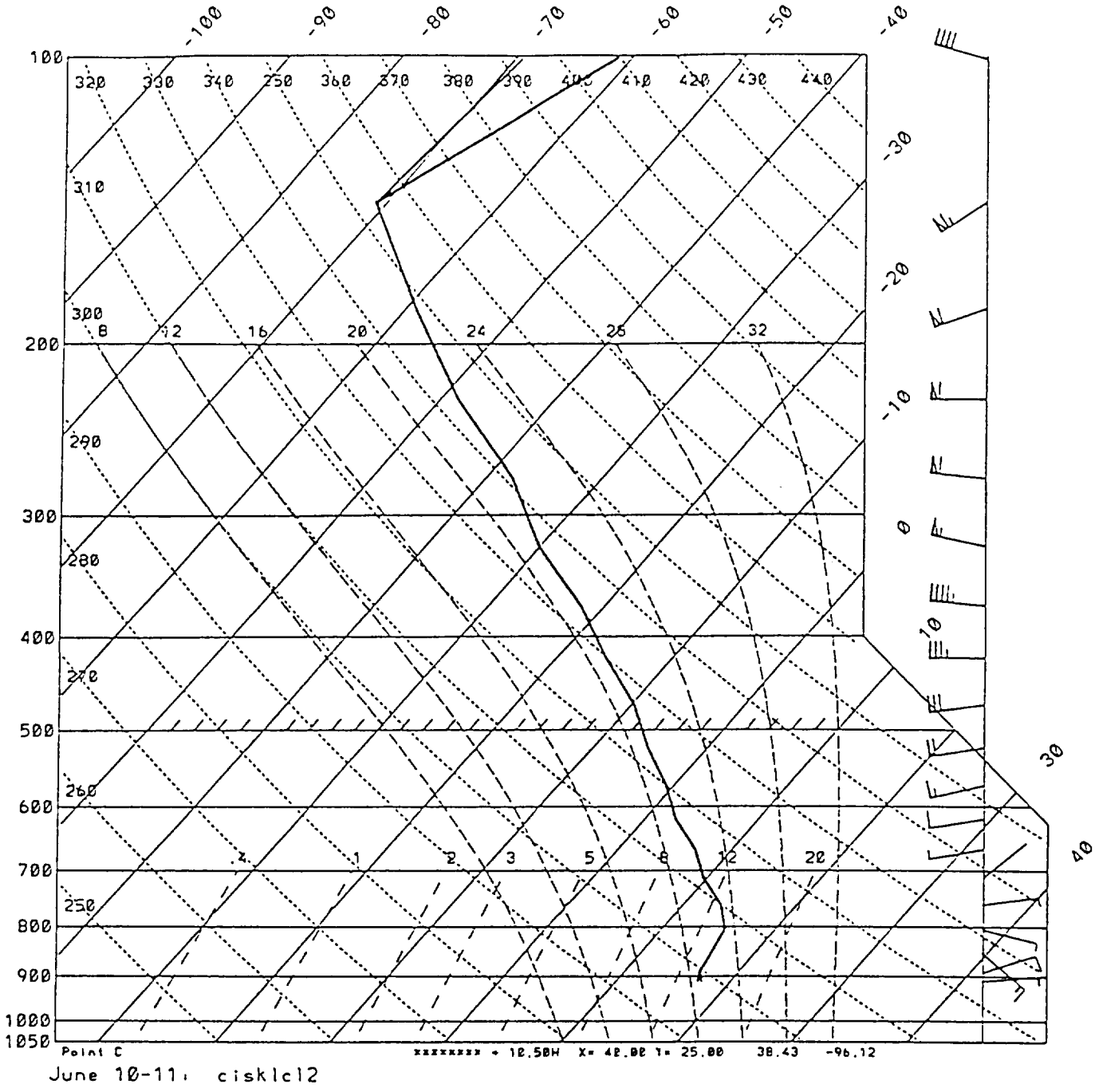

Fig. 6 Vertical sounding on a Skew-T log-P diagram from the June 10-11 squall line simulation. Sounding location is indicated by point C in Fig. 5; sounding time is 10.5 h into the simulation.